the plant journal

SEB Society for Experimental Biology

The Plant Journal (2013) doi: 10.1111/tpj.12221

SPL8 and miR156-targeted *SPL* genes redundantly regulate Arabidopsis gynoecium differential patterning

Shuping Xing[1,†], María Salinas[2,†], Antoni Garcia-Molina[1], Susanne Höhmann[1], Rita Berndtgen[1] and Peter Huijser[1,*]

[1]*Department of Comparative Development and Genetics, Max Planck Institute for Plant Breeding Research, Carl-von-Linné-Weg 10, 50829 Cologne, Germany, and*

[2]*Department of Applied Biology, University of Almería, CITE II-B, Carretera de Sacramento s/n,04120 Almería, Spain*

Received 14 March 2013; revised 16 April 2013; accepted 24 April 2013.

*For correspondence (e-mail huijser@mpipz.mpg.de).

†These authors contributed equally to this work.

SUMMARY

***SPL8* and miR156-targeted *SPL* genes are known to play an essential role in Arabidopsis anther development. Here we show that these *SPL* genes are also expressed within the developing gynoecium, where they redundantly control development of the female reproductive tract. Whereas the gynoecium morphology in the *spl8* single mutant is largely normal, additional down-regulation of miR156-targeted *SPL* genes results in a shortened style and an apically swollen ovary narrowing onto an elongated gynophore. In particular, the septum does not form properly and lacks a transmitting tract. Loss of *SPL8* function enhances the mutant phenotypes of *ett*, *crc* and *spt*, indicating a functional overlap between *SPL8* and these genes in regulating gynoecium development. Furthermore, gynoecium development of *35S:MIR156b spl8–1* double mutants shows enhanced sensitivity to a polar auxin transport inhibitor, and the expression pattern of the auxin biosynthesis gene *YUCCA4* is altered compared to wild-type. Our observations imply that *SPL8* and miR156-targeted *SPL* genes control gynoecium patterning through interference with auxin homeostasis and signalling.**

Keywords: gynoecium development, *Arabidopsis thaliana*, fertility, miR156, SBP-box gene, transmitting tissue.

INTRODUCTION

The reproductive organs within a flower are structurally and functionally among the most complex organs found in plants. This is particularly true for the female part or gynoecium formed by the carpels in the centre of the flower. Not only does this organ produce ovules, it also has to receive the male gametophytes, facilitate their germination, guide their pollen tubes, support embryo development and seed maturation, and finally enable seed dispersal. Whereas carpel and ovule identity within the flower are well explained by the ABC(D) model describing the action of several homeotic gene functions, either alone or in combination (Angenent *et al.*, 1995), the molecular genetic specification and development of the highly specialized tissues supporting the various functions mentioned above, is much less well understood. In Arabidopsis, expression of the homeotic C–class gene *AGAMOUS* determines carpel identity in the centre of the flower. Carpels appear at stage 6 of flower development in the form of a gynoecial primordium that initially commences growth as an open-ended cylinder (Ferrándiz *et al.*, 1999). Within this bi-carpellate chimney-like structure, tissue development and differentiation at subsequent stages proceed along the three principal axes, i.e. in apical–basal, medial–lateral and adaxial–abaxial directions (Ferrándiz *et al.*, 2010). Along the medial–lateral axis, two opposing placental regions start to form at stage 8 and initiate ovule primordia at stage 9. Simultaneously, endo-, meso- and exocarp layers differentiate along the adaxial–abaxial axis, with two major lateral vascular bundles perpendicular to that. At stage 10, a septum forms and the gynoecium closes when style and stigma develop apically. Within the style and septum, a transmitting tract develops along the apical–basal axis. By formation of medial repla as visible sutures partitioning the ovary wall in two valves and formation of a short basal gynophore, maturation of the receptive female organ or pistil is completed when the flower reaches anthesis at stage 13.

During fertilization, the stigma with its papillary cells is involved in adhesion and germination of the pollen, and guidance of the growing pollen tube into the transmitting

tract. This specialized tissue generates an extracellular matrix that guides the advancing pollen tubes further in the direction of the ovules embedded deeper in the organ (Lord and Russell, 2002; Balanza *et al.*, 2006; Crawford and Yanofsky, 2008). After fertilization, the ovary expands to accommodate the developing seeds and forms a silique. After ripening and lignification of the endocarp layer and the cells adjacent to the sutures connecting the valve margins to the replum, silique dehiscence enables shattering, i.e. detachment of the valves and dispersal of the mature seeds.

Genetic screens have identified several transcriptional regulators that control various aspects of Arabidopsis gynoecium development and function. The *SPATULA* (*SPT*) and *HECATE* (*HEC*) genes act in concert to regulate development of the female reproductive tract, as mutations of these genes result in improper differentiation of the transmitting tissue and alterations in the stigma and style (Alvarez and Smyth, 1999; Gremski *et al.*, 2007). In addition, specific expression of the *NO TRANSMITTING TRACT* (*NTT*) gene in the transmitting tract facilitates pollen tube growth, and this becomes inhibited when *NTT* function is lost (Crawford *et al.*, 2007). Mutation of *CRABS CLAW* (*CRC*) prevents fusion of the two carpels in the upper part of the gynoecium, and the whole organ remains shorter and wider. This phenotype is related to the function of CRC in directly or indirectly suppressing excess lateral expansion and promoting longitudinal growth of the developing carpel (Alvarez and Smyth, 1999). Gynoecium apical development is also affected by *STYLISH1* and *2* (*STY1* and *STY2*), resulting in reduction of stylar and stigmatic tissues upon loss of function, and an expansion of stylar tissue into the valve domain upon ectopic over-expression (Kuusk *et al.*, 2002). STY1 may activate *NGATHA* (*NGA1–4*) genes, or cooperate with them at the same level, in order to direct style and stigma development (Alvarez *et al.*, 2009; Trigueros *et al.*, 2009). In addition, genes such as *SHATTERPROOF1* and *2* (*SHP1* and *SHP2*), which play major roles in valve dehiscence zone differentiation (Liljegren *et al.*, 2000), may participate in gynoecium apex formation (Colombo *et al.*, 2010).

ETT is another key gene in apical–basal patterning, and probably also adaxial–abaxial gynoecium patterning, as its mutants show an increase in stylar and stigmatic regions at the expense of the ovary (Sessions and Zambryski, 1995). ETT is a member of the auxin response factor (ARF) family of transcription factors, and has been proposed to interpret auxin levels in order to specify regional domains in the developing gynoecium (Balanza *et al.*, 2006). Based on this and additional data, Nemhauser *et al.* (2000) proposed a model in which high, medium and low levels of auxin along the apical–basal axis of the early gynoecium correlate with formation of the stigma/style, ovary and gynophore, respectively. A change in this gradient causes a shift in the location of the boundaries between these parts. *ETT* and some other genes mentioned above are likely to affect gynoecium development directly or indirectly through auxin signalling. For instance, the *spt* mutant phenotype may be partially rescued by chemical inhibition of polar auxin transport (Nemhauser *et al.*, 2000). Moreover, STY1 targets *YUCCA4* (*YUC4*), which encodes an auxin biosynthetic enzyme. Therefore, *STY1*, together with *NGA* genes, may promote style specification, partly by directing auxin synthesis in the gynoecium apex (Trigueros *et al.*, 2009; Eklund *et al.*, 2010).

We have previously described how the SBP domain transcription factor encoded by *SQUAMOSA PROMOTER BINDING PROTEIN-LIKE8* (*SPL8*) acts together with other *SBP-Like* (*SPL*) genes to preserve male fertility in Arabidopsis (Xing *et al.*, 2010). Their simultaneous loss of function causes absence of pollen sacs within anthers, and we obtained some evidence that *SPL8* may affect female fertility as well (Unte *et al.*, 2003; Xing *et al.*, 2010). In male fertility, *SPL8* acts redundantly with other *SPL* genes whose transcripts are targeted by microRNAs miR156 and miR157. Here we report that *SPL8* and miR156/7-targeted *SPL* genes are also important for female fertility, and discuss the experimental evidence indicating their role in gynoecium patterning.

RESULTS

SPL8 is expressed in multiple tissues and organs during development

Consistent with its mutant phenotype, *SPL8* is expressed strongly in early anthers (Unte *et al.*, 2003; Xing *et al.*, 2010). To determine whether *SPL8* is also expressed elsewhere in the plant, we performed quantitative RT–PCR analysis of various organs. *SPL8* expression was detected weakly in seedlings and strongly in inflorescences and siliques, but virtually not at all in root, stem, rosette or cauline leaves (Figure 1a). To obtain a more detailed view during development, we introduced a *pSPL8:GUS* reporter transgene. After sampling at various developmental stages, we did not detect obvious GUS activity in 3- and 6-day-old seedlings (Figure 1b), but the trichomes of young leaves of 13-day-old seedlings clearly stained blue (Figure 1c). We did not observe a GUS signal in other leaf tissues or in roots at these stages (Figure 1b,c). During the floral transition, GUS expression was still detected in trichomes on young leaves (Figure 1d). After bolting, strong staining appeared in inflorescences (Figure 1e), primarily early anthers and gynoecia. In the latter, the GUS signal became most intense at anthesis (Figures 1f and 4a1–a5), and remained detectable in the top and bottom of the elongating siliques after fertilization (Figure 1f). This typical expression pattern raised the question of whether *SPL8* plays a role in gynoecium development.

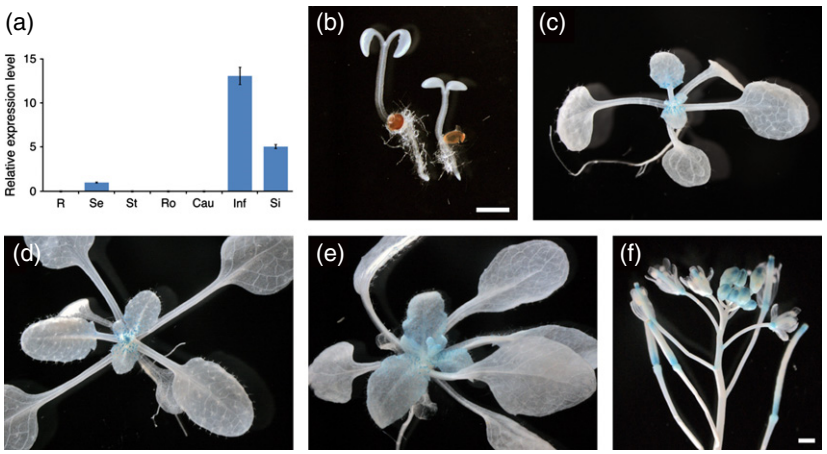

Figure 1. Dynamic expression pattern of *SPL8*.
(a) Quantitative RT–PCR analysis of *SPL8* expression in various organs. R, root; Se, seedling; St, stem; Ro, rosette leaf; Cau, cauline leaf; Inf, inflorescence; Si, silique.
(b–f) GUS staining of *pSPL8:GUS* transgenic plants at various developmental stages: (b) 3-day-old seedling (right) and 6-day-old seedling (left); (c) 13-day-old seedling; (d) 18-day-old seedling; (e) 23-day-old plant; (f) upper part of the primary inflorescence from a 35-day-old plant. Scale bars = 1 mm (b) and 1 mm (c–f).

spl8 enhances the gynoecial defects of *ett, crc, spt* and *sty1* mutants

At anthesis, the morphology of the *spl8* mutant gynoecium largely resembled that of the wild-type, but in some flowers its overall length was approximately 10% less than that of the wild-type (Figure 2a,b). To obtain information regarding a possible function for *SPL8* in gynoecium development, we crossed *spl8–1* with the *ett*, *crc*, *spt* and *sty1* mutants, respectively. The latter mutants show abnormal phenotypes in carpel fusion and/or development of the style and stigma. To avoid an effect of differences in genetic backgrounds, we used existing alleles or identified alleles in the Col background (Figure S1). The *ett* mutant (*ett–22*) used in this study has been described previously, and exhibited a weak phenotype in comparison to the original *ett–1* mutant (Pekker *et al.*, 2005), with a mis-patterned stigma/stylar region and pronounced outgrowth of the replum, but only slightly reduced valve size (Figure 2c). However, the valves decreased to less than two-thirds of the length of the gynoecium in the *ett spl8–1* double mutant and the gynophore was strikingly elongated (Figure 2d). As described above, mutation of *CRC* results in a slightly shorter but broader gynoecium that often remains split open apically. The *crc* mutant that we identified shared this phenotype (Figure 2e). However, in the *crc spl8–1* double mutant, the apical cleft caused by the lack of carpel fusion appeared to deepen in the upper part of the ovary (Figure 2f). The *spt* mutation causes narrowing of the style and a reduction in stigmatic papillae development. Within the *spt* ovary, the septum remains unfused and transmitting tissue is absent (Alvarez and Smyth, 1999). The *spt* mutant that we used showed a less severe phenotype, with only a slightly narrower style and reduced stigma (Figure 2g). Interestingly, most gynoecia within *spt sp8–1* double mutant flowers exhibited a narrower and often one-sided bent style, with a further size-reduced stigma on top (Figure 2h). The gynoecia of the *sty1* mutant that we examined also exhibited a mildly abnormal phenotype, in that only the style and stigma were slightly mis-patterned (Figure 2i), and some papilla cells appeared to stick together (Figure 2k). Obviously, this adherence tendency was enhanced in *sty1 spl8–1* double mutants (Figure 2l). Furthermore, the gynoecia of *sty1 spl8–1* double mutant flowers remained generally smaller and their stigma appeared to develop later compared to those of the *sty1* single mutant (Figure 2j).

In summary, all the observations described above indicate that mutation of *SPL8* may enhance the mutant phenotypes of several genes that are already known to play important roles in gynoecium development. These results strongly suggest that *SPL8* participates in related pathways to regulate gynoecium development.

Down-regulation of miR156-targeted *SPL* genes in the *spl8–1* mutant background dramatically changes gynoecial morphology

As described above, mutation of *SPL8* alone only slightly affected the size and shape of a flower stage 13 gynoecium (Figure 3a,b). However, flowers of *35S:MIR156b* transgenic plants, in which miR156-targeted *SPL* genes are down-regulated (Xing *et al.*, 2010), formed a clearly shorter gynoecium, although the overall shape did not change much (Figure 3c). This observation indicated that at least one or more of the miR156-targeted *SPL* genes is required for normal gynoecium development. In a previous study, we demonstrated that *SPL8* and miR156-regulated *SPL* genes share some redundant functions in anther development (Xing *et al.*, 2010). To determine whether these genes also act redundantly to control gynoecium development, we focused on the gynoecium of *35S:MIR156b spl8–1* double mutant flowers. The overall length of the gynoecium was found to be slightly shorter compared to *35S:MIR156b* transgenic flowers, but the shape of the gynoecium was

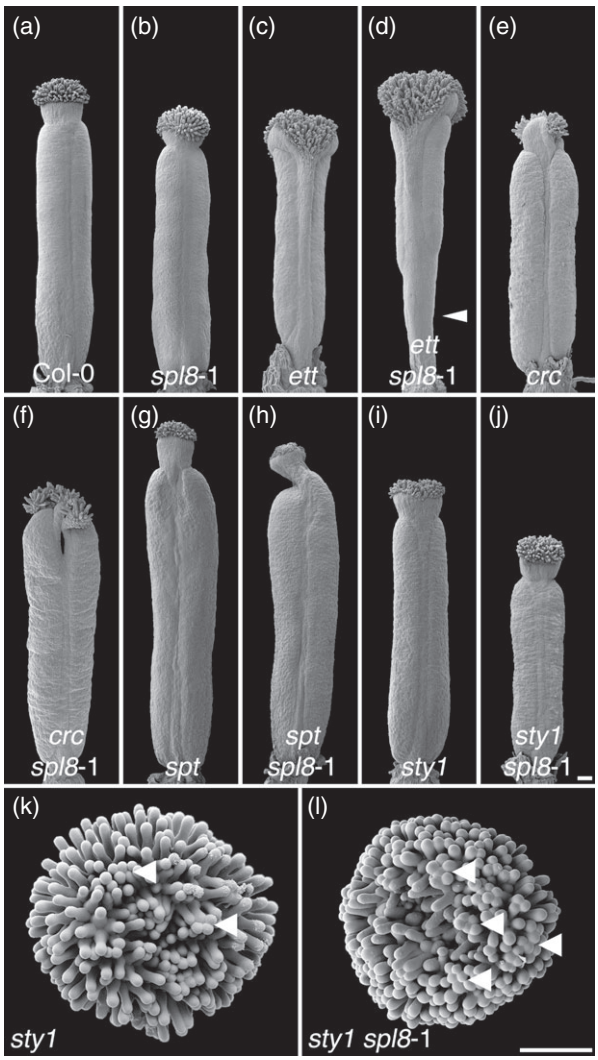

Figure 2. Scanning electron micrographs of gynoecia of wild-type, *spl8–1*, and combinations between *spl8–1* and various gynoecium mutants
(a) Col–0.
(b) *spl8–1* mutant.
(c) *ett* gynoecium exhibiting a weak mutant phenotype in stigmatic and stylar regions.
(d) *ett spl8–1* gynoecium with an elongated gynophore (arrowhead).
(e) *crc* mutant gynoecium with reduced stigmatic papillae and split style.
(f) *crc spl8–1* double mutant, with a deep split on the upper part of the ovary.
(g) *spt* mutant gynoecium with less developed stigma.
(h) *spt spl8–1* gynoecium with a bent style.
(i) *sty1* mutant gynoecium, with stigmatic tissue slightly growing towards the centre.
(j) *sty1 spl8–1* gynoecium with randomly growing stigmatic papillae on top.
(k) Top view of the *sty1* stigma at high magnification, showing some fused papillae cells (arrowheads).
(l) Top view at high magnification of the *sty1 spl8–1* stigma, exhibiting more fused papillae cells (arrowheads).
(a–h) Stage 13 gynoecia; (i–l) stage 12 gynoecia. Scale bars = 100 μm (a–j) and 100 μm (k, l).

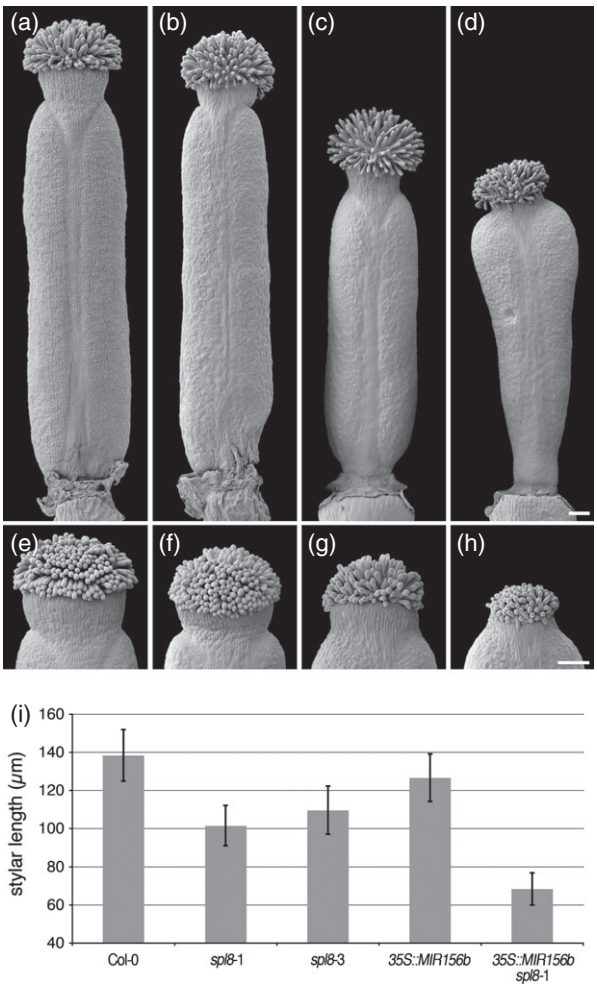

Figure 3. Morphology and style length of wild-type, *spl8–1*, *35S:MIR156b* and *35S:MIR156b spl8–1* gynoecia.
(a) Col–0.
(b) *spl8–1* mutant.
(c) *35S:MIR156b* transgenic gynoecium, which is one-third shorter than wild-type.
(d) *35S:MIR156b spl8–1* gynoecium, showing a reduced style and an ovary that is wider at the top and narrower at its base.
(e) Col–0, zoomed in on stylar region like in (f–h).
(f) *spl8–1* mutant, in which the style is significantly shorter compared to wild-type.
(g) *35S:MIR156b* stylar region.
(h) *35S:MIR156b spl8–1* gynoecium, displaying a very short style.
(i) Quantification of style length of stage 12 gynoecia (30 gynoecia were measured from each genotype).
(a–d) Stage 13 gynoecia; (e–h) stage 12 gynoecia. Scale bars = 100 μm (a–d) and 100 μm (e–h).

dramatically changed, with a swollen upper part and an increasingly narrower basal part. In addition, the style was severely shortened (Figure 3d). In fact, at flower stage 12, the style of *spl8* mutants also appeared shorter than that of wild-type (Figure 3e–i), although its length appeared to have caught up with that of the wild-type at anthesis, at least partially (stage 13). Taken together, these data indicate that, in addition to *SPL8*, miR156-targeted *SPL* genes contribute to gynoecium development along the apical–basal axis, either alone or together.

SPL8 and several miR156-targeted *SPL* genes are expressed in overlapping domains throughout gynoecium development

According to publicly available microarray expression data from the AtGenExpress developmental series (Schmid *et al.*, 2005), several miR156-targeted *SPL* genes are strongly expressed in flower stage 12 carpels. To obtain a more detailed picture of their expression pattern, we selected *SPL2*, *SPL10*, *SPL11*, *SPL6* and *SPL13*, and generated promoter–GUS reporter transgenic lines referred to as *pSPL2:GUS*, *pSPL10:GUS*, *pSPL11:GUS*, *pSPL6:GUS* and *pSPL13:GUS*, respectively. For comparison, a *pSPL8:GUS* line was analysed in parallel. After staining, we observed GUS expression for all these lines in flowers at various developmental stages. In *pSPL8:GUS* flowers, obvious GUS staining was detected in early anthers, and a weak signal appeared in the apex of gynoecia at stage 9 (Figure 4a1). At later stages, staining had disappeared from anthers, but had increased in gynoecia and expanded downwards to the regions that give rise to the style, replum and septum (Figure 4a1–a4). At anthesis, staining of the gynoecium had become confined to the upper region below the style (Figure 4a5). In *pSPL2:GUS* flowers at stage 9, GUS staining was observed in young gynoecia as well as sepals (Figure 4b1). During subsequent stages 10–13, the signal increased strongly in the upper part of the gynoecium, including the apical and stylar regions, and persisted in sepals. At stage 12, additional staining appeared in stamen filaments, including anthers at stage 13 (Figure 4b2–b5). For both *pSPL10:GUS* and *pSPL11:GUS*, the staining pattern largely resembled that of *pSPL2:GUS* (Figure 4c1–d5 and d1–d5), although the GUS signal extended further downwards in stage 10 gynoecia (Figure 4c2 and d2) and appeared somewhat later in filaments of *pSPL11:GUS* stamens (Figure 4d5). Strong GUS staining was observed in *pSPL6:GUS* gynoecia through all examined stages (9–13), but became more

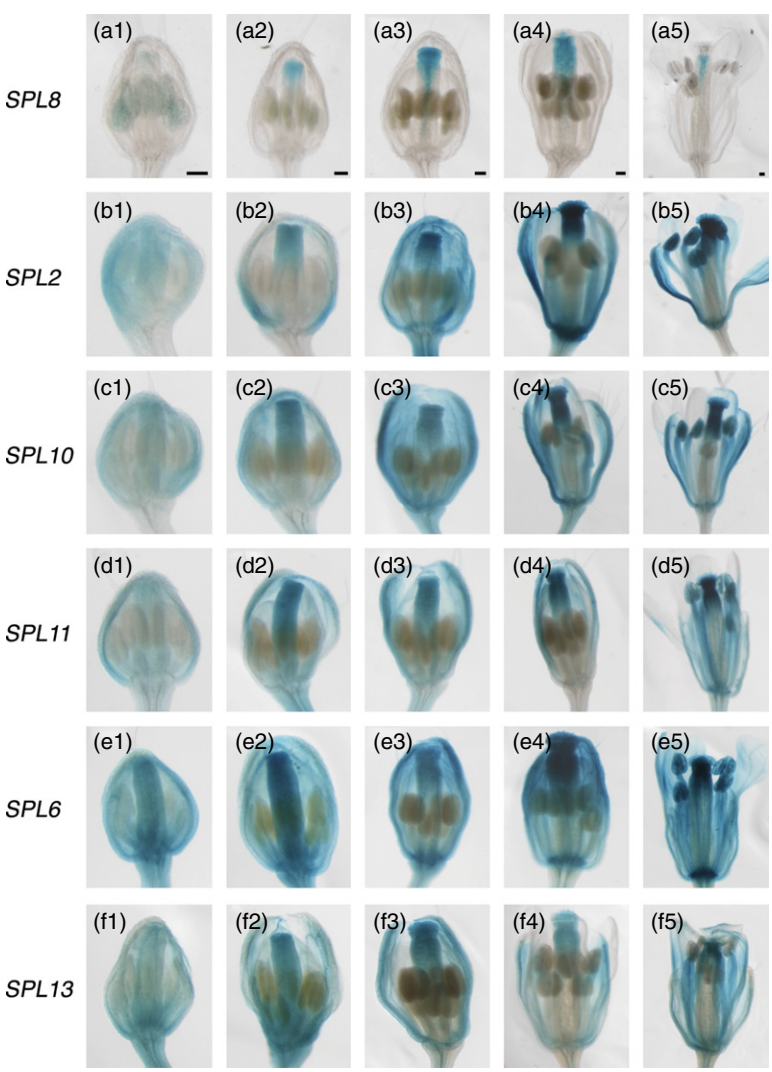

Figure 4. Expression pattern of various *SPL* promoter:GUS reporter transgenes in stage 9–13 flowers.
(a1–f1) Stage 9. (a2–f2) Stage 10. (a3–f3) Stage 11. (a4–f4) Stage 12. (a5–f5) Stage 13.
(a1–a5) *pSPL8:GUS*. (b1–b5) *pSPL2:GUS*. (c1–c5) *pSPL10:GUS*. (d1–d5) *pSPL11:GUS*. (e1–e5) *pSPL6:GUS*. (f1–f5) *pSPL13:GUS*.
Scale bars = 100 μm, and apply to all images in that column.

confined to the upper part (Figure 4e1–e5). A persistent GUS signal was also detected in sepals and petals as well as in filaments and mature anthers of stage 13 flowers (Figure 4e5). Expression of the GUS reporter in *pSPL13:GUS* flowers resembled that of *pSPL11:GUS*, except for a weak signal detected in early anthers (Figure 4f1) but not mature anthers (Figure 4f5).

Taken together, these data show that *SPL8* and the selected miR156-targeted *SPL* genes have overlapping expression domains in the gynoecium at various developmental stages, corroborating the idea that they redundantly regulate development of this organ.

Female fertility test in *SPL* mutants

Many known gynoecial mutants suffer from a female fertility problem. We therefore examined the fertility of some available *spl* mutants, or combinations thereof, by manual pollination using the wild-type as a pollen donor. The data in Table 1 show that mutation of only *SPL8* neither significantly affected ovule number nor seed set when compared to wild-type. However, *35S:MIR156b* transgenic ovaries produced only half the number of ovules found in the wild-type, and accordingly set less seeds per silique. However, the efficiency of seed production after cross-pollination appeared somewhat reduced, i.e. 88.5% compared to 98.3% for wild-type. The triple mutants *spl8–1 spl2–1 spl15–1*, *spl8–1 spl9–1 spl15–1* and *spl2–1 spl9–1 spl15–1* and the quadruple mutant *spl8–1 spl2–1 spl9–1 spl15–1* showed a more or less similar seed set, between that of wild-type and the *35S:MIR156b* transgenic line. Remarkably, however, combining *spl8–1* and *35S:MIR156b* dramatically reduced seed set to a mean of only 2.5 seeds per silique. Whereas the additional mutation of *SPL8* only slightly further reduced the ovule number compared to the *35S:MIR156b* transgene alone, the efficiency of seed production in the double mutant decreased to approximately one-tenth that of wild-type, i.e. 10.9%. These data strongly suggest that *SPL8* and miR156-targeted *SPL* genes are involved in determining female fertility.

Table 1 Female fertility test of various *spl* mutants

Genotype	Ovules per ovary[b]	Seeds per silique[a,b]	Seed set efficiency (%)
Col–0	64.0 ± 4.8	62.9 ± 5.2	98.3
spl8–1	67.5 ± 4.2	65.5 ± 11.9*	96.9
spl8–1 spl2–1 spl15–1	NA	40.9 ± 13.8*	NA
spl8–1 spl9–1 spl15–1	NA	39.7 ± 16.8*	NA
spl8–1 spl2–1 spl9–1 spl15–1	NA	42.3 ± 7.5*	NA
spl2–1 spl9–1 spl15–1	NA	40.1 ± 12.1*	NA
35S::MIR156b	28.8 ± 3.6*	25.5 ± 6.1*	88.5
35S::MIR156b spl8–1	23.1 ± 3.2*	2.5 ± 2.9*	10.9

[a]Determined after cross-pollination with wild-type pollen.
[b]Mean values with standard deviation (n = 7–23).
*Significantly different from Col–0 at $P < 0.01$ (Welch's t test).

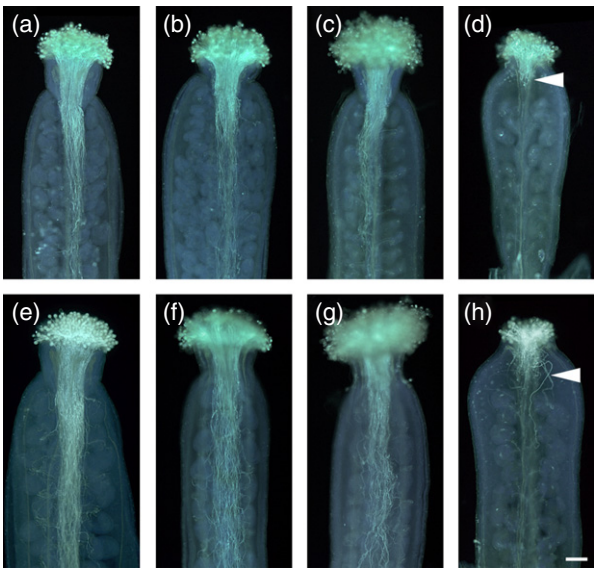

Figure 5. Pollen tube growth in wild-type, *spl8–1*, *35S:MIR156b* and *35S:MIR156b spl8–1* gynoecia.
Wild-type Col–0 as pollen donor 6 h after pollination (a–d) and 24 h after pollination (e–h).
(a, e) Col–0 gynoecia: pollen tubes grow normally into the ovary.
(b, f) *spl8–1* mutant gynoecia: the pattern of pollen tube growth is similar to that of wild-type in (a) and (e).
(c, g) *35S:MIR156b* transgenic gynoecia: the growth of pollen tubes into ovary appears slightly reduced.
(d, h) *35S:MIR156b spl8–1* plant: pollen germinated on stigma, but tube growth appeared severely hampered, with only a few growing tubes entering the ovary and following random paths (arrowheads).
Scale bar = 100 μm.

Pollen tube penetration into the ovary is impaired in *35S:MIR156b spl8* plants

To obtain a better understanding of what may have caused the low efficiency of seed production in *35S:MIR156b spl8–1* double mutants, we repeated the pollination experiment. This time, we collected the pistils at 6, 24 and 48 h after manual pollination with wild-type pollen, and stained them with aniline blue to visualize the developing pollen tubes. At 6 h after pollination, the pollen tubes in the wild-type had grown directionally into the ovary chamber and down along the transmitting tract for over half the length of the pistil (Figure 5a). Similar progression of the pollen tube growth was observed in *spl8–1* mutant and *35S:MIR156b* transgenic pistils (Figure 5b,c). However, the tubes from pollen germinated on the stigma of *35S:MIR156b spl8–1* double mutants remained at the stylar region (Figure 5d). At 24 h after pollination, the density of pollen tubes half way along the transmitting tract had strongly increased in both wild-type and *spl8–1* mutant pistils (Figure 2e,f), and many already reached the bottom of the ovary chamber. The pollen tube density, although lower, had also

increased in *35S:MIR156b* transgenic pistils (Figure 5g), but only some pollen tubes reached the base of ovary. Overall, it appears that pollen tubes grew slightly less well through the *35S:MIR156b* transmitting tract. However, at this time point, in clear contrast to wild-type and both parental lines, only a few pollen tubes managed to enter the ovary chamber of the *35S:MIR156b spl8–1* double mutant pistil (Figure 5h). Moreover, their length lagged far behind those in wild-type, and their direction of growth was poorly or even unguided (Figure 5h). Even 48 h after pollination, the situation for pollen tube growth in *35S:MIR156b spl8–1* pistils had not improved much. This phenotype is consistent with the results of the female fertility test, where at best only a few seeds were obtained from cross-pollinated *35S:MIR156b spl8–1* transgenic flowers. Our observations indicate that pollen grains on the stigma of *35S:MIR156b spl8–1* pistils may germinate normally, but then appear unable to penetrate into the ovary chamber properly. A few pollen tubes appear to reach the ovules along random paths.

35S:MIR156b spl8–1 gynoecium lacks the transmitting tissue

To find a reason why pollen tubes were unable to penetrate the ovaries of the *35S:MIR156b spl8–1* pistils properly, we prepared cross-sections through the gynoecium (Figure 6a). In wild-type, the stylar region was fully fused and centrally closed (Figure 6b). The intracellular matrix of the central tissue clearly stained with Alcian blue, indicating the presence of acidic polysaccharides required to support pollen tube growth (Sessions and Zambryski, 1995). At a comparable position, the short style of *35S:MIR156b spl8–1* gynoecia remained slightly open in the centre, although some medial, adaxial opposing and expanding epidermal cells appeared to adhere (Figure 6c). Cross-sections over the full length of the wild-type ovary showed a fully developed septum with dark, Alcian blue-stained transmitting tissue in the middle (Figure 6d) gradually decreasing towards the base of the ovary (Figure 6f). In clear contrast, however, a gap remained between the tissue protrusions that are arranged medially in the upper part of the *35S:MIR156b spl8–1* mutant ovary and are assumed to form a septum (Figure 6e). The absence of Alcian blue staining indicated the lack of transmitting tissue formation (Figure 6e). A closed septum was found in the mid and basal part of the double mutant ovary, but Alcian blue-positive transmitting tissue remained undetectable (Figure 6g). These observations indicate that *35S:MIR156b spl8–1* pistils do not develop a transmitting tract along their apical–basal axis that is capable of supporting and guiding pollen tube growth into the ovary. In addition, and particularly in the upper ovarian region, ovules were occasionally found displaced towards a more lateral position on the inner (adaxial) epidermis of carpels

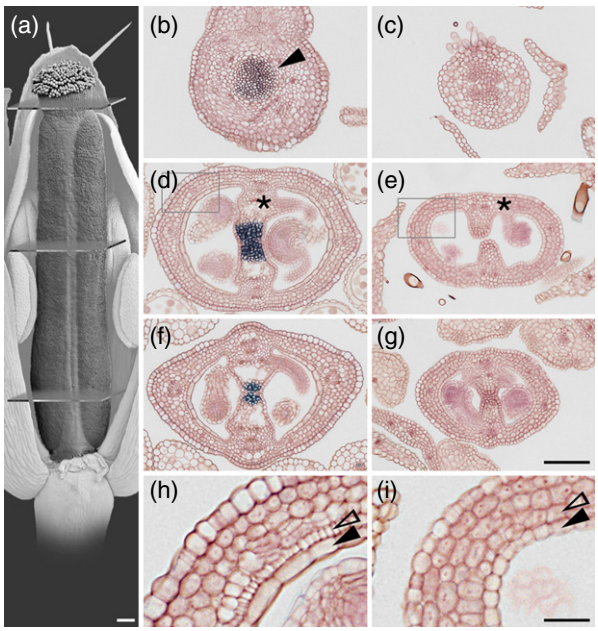

Figure 6. Transverse sections of stage 12 gynoecia of wild-type and *35S:MIR156b spl8–1* plants.
(a) Wild-type gynoecium indicating planes of section. (b,d,f,h) Col–0. (c,e,g,i) *35S:MIR156b spl8–1*.
(b, c) Sections from the style. Transmitting tissue is observed centrally in styles of wild-type (b, arrowhead), but not of *35S:MIR156b spl8–1* gynoecia (c).
(d, e) Sections from upper parts of the ovary, showing the transmitting tissue in the septum of wild-type (d), while the outgrowth from the carpel margins remains unfused in *35S:MIR156b spl8–1* plants and transmitting tissue is absent (e). Asterisks indicate the ovule attachment site.
(f, g) Sections from lower parts of the gynoecia. Transmitting tissue still exists in the wild-type gynoecium (f) but is absent in *35S:MIR156b spl8–1* gynoecia, although the outgrowth from margins of the carpel in the centre appears to fuse at this level (g).
(h, i) Enlargement of boxed areas from (d) and (e), respectively, to show the size and shape of the endocarp sub-layers *a* (closed arrowhead) and *b* (open arrowhead).
Scale bars = 100 μm (a), 100 μm (b–g) and 25 μm (h, i).

(Figure 6e). Trichomes were observed developing from the inner epidermis in the upper part of the double mutant ovary (Figure S2.). Most likely related was the striking change in cell morphology of the inner epidermal and subepidermal layer of the mutant valve compared to wild-type. These endocarp layers a and b (en*a* and en*b*), respectively, were obviously distinct in wild-type ovary cross-sections. Although the cells in *35S:MIR156b spl8–1* mutant ovaries were similar in shape (Figure 6i), wild-type cells of the en*a* layer were enlarged and elongated periclinally, and those of the en*b* layer were smaller (Figure 6h). In wild-type, en*a* and en*b* originate from a periclinal division in the endocarp, and comparing the number of cell layers between the inner and outer epidermis indicated that this division may have failed in the *35S:MIR156b spl8–1* mutant. Taken together, the histological data suggest that gynoecial tis-

sue differentiation along the adaxial–abaxial axis is controlled by *SPL8* and miR156-targeted *SPL* genes.

35S:MIR156b spl8–1 gynoecia are hypersensitive to NPA

Previous studies on mutants impaired in auxin homeostasis or signalling, as well as experiments with chemical inhibitors of polar auxin transport demonstrated a profound effect of auxin on gynoecium patterning. When plants are sprayed with 1–*N*–naphthylphthalamic acid (NPA), an inhibitor of polar auxin transport, the most apparent effect in the developing flower is on the apical–basal patterning of the gynoecium, including style and gynophore elongation, with a concomitant decrease in ovary size (Nemhauser *et al.*, 2000). The gynoecium in *35S:MIR156b spl8–1* double mutant flowers exhibited a short style, an elongated gynophore and a reduced ovary, indicating an apical–basal patterning defect, and thus possibly disturbed auxin homeostasis or signalling. We therefore examined the response of the *35S:MIR156b spl8–1* transgenic line to NPA. According to the literature, the gynoecia of developing wild-type flowers sprayed with 100 μmol NPA are affected to different extents (Nemhauser *et al.*, 2000). Consistently, when compared to mock-treated plants, we observed that, 12 days after spraying, 48.6% of the NPA treated wild-type gynoecia showed only slight style and gynophore elongation and 45.7% showed significant style and gynophore elongation (Figure 7a–c). Severely affected, and in some cases even valveless, pistils were observed in 5.7% of the NPA-treated wild-type flowers (Figure 7d). However, the visible NPA effect on *35S:MIR156b spl8–1* double mutant flowers was much more dramatic (Figure 7e–h). Compared to mocked-treated plants (Figure 7e,f), the valves were reduced to half their normal size in 38.6% of the NPA-treated mutant gynoecia. An additional 47.1 and 14.3% showed gynoecia with very small or nearly absent valves, respectively (Figure 7g,h). Compared to wild-type, the developing double mutant gynoecia responded more strongly to NPA and thus appeared to be more sensitive to alterations of polar auxin transport during apical–basal patterning. These observations suggest that *SPL8*, together with miR156-targeted *SPL* genes, may control gynoecium patterning through auxin signalling or homeostasis.

Figure 7. Morphology of NPA-treated wild-type and *35S:MIR156b spl8–1* gynoecia.
(a–d) Col–0. (e–h) *35S:MIR156b spl8–1* plants.
(a, e) Mocked-treated gynoecia.
(b–d, f–h) Gynoecia treated with 100 μmol NPA.
Scale bar = 100 μm.

The *YUC4* expression pattern and *HEC2* expression level are altered in *spl* mutants

YUC4 is an auxin biosynthesis gene that is involved in gynoecium development (Eklund *et al.*, 2010). To further test the possibility that altered auxin homeostasis underlies the *35S:MIR156b spl8–1* gynoecial defects, we crossed a homozygous *pYUC4:GUS* reporter line with homozygous *spl8–1* mutant and the *35S:MIR156b* transgenic line, respectively. Thereafter, *pYUC4:GUS* expression was comparatively analysed in the inflorescences and flowers of double homozygous plants. The *pYUC4:GUS* transgene in a wild-type background exhibits apical expression in gynoecia from young to mature flowers (Figure 8a–e). The strength of the GUS signal progressively increased from flower stage 9–13, and showed an annular expression domain in a top view of the gynoecium (Figure 8b–e). In addition, a weak signal appeared in the sepals of these flowers, and staining of the filaments was observed in stage 13 flowers (Figure 8b–e). In contrast to wild-type, GUS signal in *spl8–1* mutant gynoecia appeared later (Figure 8f–j). No staining was detected in flower stage 9, and only a faint signal appeared at stage 10 (Figure 8g,h). Most strikingly, GUS expression remained divided over two lateral domains instead of forming a closed annulus or disc (Figure 8h–j). To some extent, this alteration in expression was also observed in the *35S:MIR156b* transgenic line, although the first appearance of a GUS signal in the gynoecium apex remained largely unchanged (Figure 8k–o). These results indicate that normal function of both *SPL8* and miR156-targeted *SPL* genes

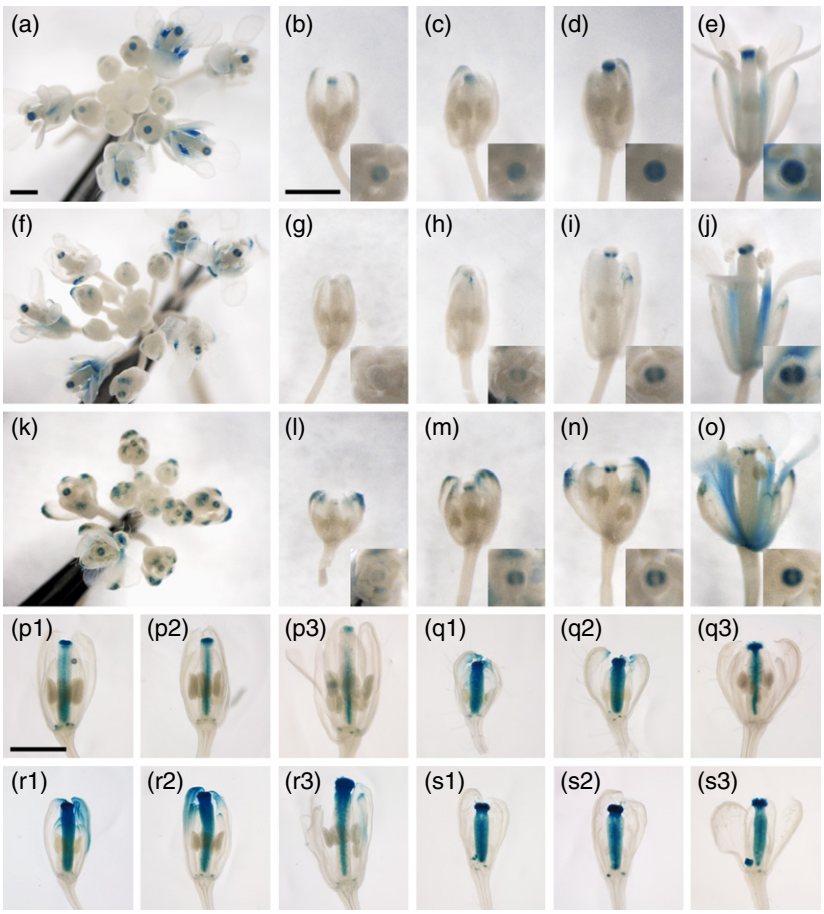

Figure 8. Analysis of *pYUC4:GUS* and *pHEC2:GUS* expression in *spl* mutants.
For comparison of GUS expression, primary inflorescences harbouring *pYUC4:GUS* in various genotypes were stained for 8 h, whereas those harbouring *pHEC2:GUS* were stained for 11 h.
(a–e) *pYUC4:GUS* in Col–0; (f–j) *pYUC4:GUS* in the *spl8–1* mutant; (k–o) *pYUC4:GUS* in the *35S:MIR156b* transgenic line. (b, g, l) Stage 9 flowers; (c, h, m) stage 10 flowers; (d, i, n) stage 12 flowers; (e, j, o) stage 13 flowers.
(p1–p3) *pHEC2:GUS* in Col–0; (q1–q3) *pHEC2:GUS* in the *35S:MIR156b* transgenic line. (r1–r3) *pHEC2:GUS* in the *spl8–1* mutant background. (s1–s3) *pHEC2:GUS* in *35S:MIR156b spl8–1* plants. (p1, q1, r1, s1) Stage 10 flowers; (p2, q2, r2, s2) stage 11 flowers; (p3, q3, r3, s3) stage 12 flowers. Scale bars = 1 mm (a,f,k), 1 mm (b–e, g–j, l–o) and 1 mm (p1–s3).

is required for proper expression of *YUC4* in gynoecium development.

We also examined the expression of *HEC2* as a representative of the *HECATE* genes affecting transmitting tissue formation. We crossed a *pHEC2:GUS* reporter transgene into the *35S:MIR156b spl8–1* double mutant. The wild-type *pHEC2:GUS* line showed GUS signal in all flower buds, where it remained confined mainly to the gynoecium with an apical intensity maximum (Figure S3). Strikingly, this GUS staining faded as the flower matured (Figure 8 p1–p3). However, a clearly increased GUS signal intensity was observed in the *35S:MIR156b spl8–1* double mutant. Also the *spl8* and *35S:MIR156b* parental lines showed a significantly elevated expression level (Figure S3). This strong GUS signal was detected in entire young flower buds, indicating that *HEC2* may be ectopically expressed in the *35S:MIR156b spl8–1* double mutant, although we cannot rule out the possibility that these ectopic signals result from diffusion out of the very strongly stained gynoecium (Figure S3). Most obviously, these *spl* mutant gynoecia maintained the strong GUS signal at later developmental stages (Figure 8 q1–s3), but it had already weakened in the wild-type (Figure 8 p1–p3). These expression data suggest that *SPL* genes repress *HEC* genes that may also be involved in auxin signalling in gynoecium development.

By affecting *YUC4* and *HEC2* expression, *SPL8* and miR156-targeted *SPL* genes appear to play a complex role in patterning the developing gynoecium by interfering with auxin signalling and homeostasis.

DISCUSSION

SPL genes have previously been shown to play important roles in several plant developmental processes, such as leaf development and plastochron determination (Moreno *et al.*, 1997; Wang *et al.*, 2008), phase transitions (Huijser and Schmid, 2011) and male fertility (Unte *et al.*, 2003; Xing *et al.*, 2010). The data presented here reveal a role for *SPL* genes in development of the gynoecium, thereby controlling female fertility.

SPL genes affect apical–basal patterning of the gynoecium

35S:MIR156b spl8–1 mutant flowers produce short gynoecia with a reduced valve region. This phenotype is much more severe than that of the *spl8–1* and *35S:MIR156b*

single mutants (Figure 3a–d), suggesting that *SPL8* and the miR156-targeted *SPL* genes regulate gynoecium apical–basal patterning redundantly. The overlapping expression patterns of *SPL8* and several miR156-targeted *SPL* genes in various developmental stages of the gynoecium (Figure 4) further support such a hypothesis. Several previously studied genes known to affect apical–basal patterning of the gynoecium in particular include *ETT*, *CRC*, *SPT* and *STY1*. *ETT* encodes an auxin-responsive transcription factor (ARF3) (Sessions *et al.*, 1997), and its mutation causes an enlargement of the stigma and style regions and an elongation of the gynophore at the expense of the ovary (Sessions and Zambryski, 1995). Using a weak *ett* allele, we demonstrated that mutation of *SPL8* enhances the *ett* mutant phenotype, suggesting that *SPL8* and *ETT* interact synergistically to regulate ovary formation. Interestingly, *ETT* negatively regulates the expression of *SPT*, which encodes a bHLH transcription factor family member, and the mutant phenotype of *ett* may be rescued by mutating *SPT* (Alvarez and Smyth, 1998; Heisler *et al.*, 2001). Consistently, an ectopic *pSPT:GUS* signal was observed in the apical region of the *ett* mutant gynoecium. Moreover, this alteration showed a dramatic enhancement upon additional mutation of *SPL8* (Figure S4), suggesting that SPL8 either promotes *ETT* expression or represses *SPT* expression. However, although suppression of the *spt* phenotype is therefore expected following mutation of *SPL8*, we actually observed a slight enhancement. One explanation for this apparent inconsistency may be that *SPL8* regulates additional factors that interact synergistically with *SPT*. Genetic evidence indicates that *SPT* also shares some functional redundancy with *CRC* in suppressing the radial growth of gynoecia while promoting their longitudinal growth (Alvarez and Smyth, 1999). Again, our double mutant analysis showed that mutation of *SPL8* enhances the *crc* mutant phenotype, and thus *SPL8* and *CRC* share some functional redundancy. Another important regulator in gynoecium patterning is STY1, which targets genes such as *YUC4* that are involved in auxin biosynthesis (Eklund *et al.*, 2010). *STY1* interacts genetically with *SPT* and possibly *CRC* as well (Kuusk *et al.*, 2002). Further genetic analysis suggests that *STY1* and *SPT* regulate gynoecium apical–basal patterning in the same pathway (Sohlberg *et al.*, 2006). Loss of *SPL8* function increased the number of fused papillae cells found in *sty1* mutant stigmas (Figure 2k,i), indicating that *SPL8* and *STY1* may also share some redundancy in regulating stigma formation. Taken together, *SPL8* and miR156-tageted *SPL* genes regulate apical–basal patterning of the gynoecium, either as part of the pathways defined by *ETT*, *SPT*, *CRC* and *STY1* or in parallel pathways that share functional redundancy with the *ETT*/*SPT*/*CRC*/*STY1* dependent pathways.

SPL genes are required for septum development and transmitting tract formation

Our pollination experiments demonstrated that female fertility is reduced dramatically in *35S:MIR156b spl8–1* double mutant flowers (Table 1). However, when manually pollinated with wild-type pollen, a few seeds developed in the siliques of *35S:MIR156b spl8–1* mutant flowers in a position-independent manner, i.e. not limited to apical or basal parts within the ovary. These data imply that, although reduced in number, the ovules of *35S:MIR156b spl8–1* gynoecia are still functional. Instead, the observed reduced female fertility of the double mutant was due to an abnormal septum and the absence of transmitting tissue to support pollen tube growth into the ovary. Similarly, *crc* and *spt* mutant gynoecia also form abnormal septa lacking a transmitting tract (Alvarez and Smyth, 1999), and, as concluded above, *SPL8* and miR156-targeted *SPL* genes appear to genetically interact with *CRC* and *SPT*, suggesting that these genes function together in regulating septum and transmitting tract formation.

The SPT protein appears able to dimerize with HEC bHLH transcription factors (Gremski *et al.*, 2007). When simultaneously mutated, *HEC1*, *HEC2* and *HEC3* causes loss of the transmitting tract. Interestingly, *HEC2* was found to be significantly up-regulated in *35S:MIR156b spl8–1*, indicating that normal expression of *HEC* genes requires these *SPL* genes, and implying that *SPL8*, miR156-targeted *SPL* genes, *SPT* and *HEC* genes function in the same pathway when regulating transmitting tract development.

NTT encodes a C2H2/C2HC zinc finger transcription factor, and is specifically expressed in the transmitting tract. Mutation of *NTT* causes failure to develop a transmitting tract and impairs pollen tube growth, thus affecting female fertility. Recently, NTT and HEC were found to regulate expression of *HALF FILLED* (*HAF*), a gene encoding another bHLH transcription factor and sharing functional redundancy with the closely related *BR ENHANCED EXPRESSION 1* and *3* (*BEE1* and *BEE3*) genes (Crawford and Yanofsky, 2011). In gynoecia of the *haf bee1 bee3* triple mutant, the septum remains unfused and a functional transmitting tract is absent, again similar to what we observed in *35S:MIR156b spl8–1* double mutant gynoecia. The relationship among the *SPL* genes and the *NTT*, *HAF*, *BEE1* and *BEE3* genes remains to be determined.

Do *SPL* genes influence auxin homeostasis and responsiveness?

Many reports have provided evidence that auxin plays a substantial role in gynoecium development, and led Nemhauser *et al.* (2000) to propose that a gradient of auxin determines apical–basal patterning of the gynoecium.

According to this hypothesis, a high level of auxin in the apical region promotes stigma and style formation, whereas intermediate and low levels of auxin specify the ovary and gynophore, respectively. We found that gynoecia of *35S:MIR156b spl8–1* plants were more sensitive to NPA than those of wild-type, suggesting that *SPL8* and miR156-targeted *SPL* genes influence auxin homeostasis or cellular responsiveness during gynoecium development. Further support is provided by our *pYUC4:GUS* analyis data, which revealed altered expression patterns of this auxin biosynthesis gene in *spl8–1* and *35S:MIR156b* mutant gynoecia. The late initiation of *YUC4* expression in the apical part of the *spl8* mutant gynoecium may contribute to the observed delay in style development (Figure 3).

In addition, our combinatorial mutation analysis demonstrated that *SPL8* and miR156-targeted *SPL* genes genetically interact with *ETT*, *CRC*, *SPT* and *STY1*, all genes that have been reported to be involved in auxin homeostasis or responsiveness. Therefore, *SPL8* and miR156-targeted *SPL* genes are also likely to be involved in the auxin signalling pathway determining apical–basal patterning of the gynoecium. Strikingly, styles of *35S:MIR156b spl8–1* double mutant gynoecia were short and their gynophores were elongated. According to the auxin gradient model, this may be explained by assuming either impaired production and/or accumulation of auxin, or a lowered responsiveness to auxin in the double mutant gynoecial apex. In addition, the products of these *SPL* genes repress *HEC* genes that may also be required for proper transmitting tract development, a process that also involves *CRC*, *ETT* and *SPT* genes.

In recent years, miR156-trageted *SPL* genes have attracted interest, particularly due to their role in the vegetative/reproductive phase change (Huijser and Schmid, 2011). It will be interesting to determine in future studies whether their concomitant effect on leaf heteroblasty relates to their role in reproductive organ development.

EXPERIMENTAL PROCEDURES

Plant materials and growth conditions

Arabidopsis thaliana ecotype Columbia (Col–0) was used as the wild-type, and all mutants and transgenic lines were in the Col–0 background. Seeds for *sty1*, *crc*, *ett* and *spt* were obtained from the Nottingham Arabidopsis Stock Centre (http://arabidopsis.info/; respective catalogue numbers N125439, N830061, N675095 and N871790). *spl8* single mutants (Unte *et al.*, 2003), the *35S:MIR156b* transgenic line (Schwab *et al.*, 2005) and the *35S:MIR156b spl8–1* double mutant (Xing *et al.*, 2010) have been described previously. Prior to sowing, seeds were imbibed and stratified for 2-4 days in the dark at 4°C. Plants were grown on pre-fertilized soil (type ED73; Einheitserde Werkverband e.V., Sinntal, Germany, http://www.einheitserde.de/) in the greenhouse at 21–23°C under long-day conditions (16 h light). For comparative experiments, plants were grown in parallel under the same conditions, and material for gene expression studies was harvested at the same time points.

Constructs and plant transformation

To generate GUS reporter constructs, fragments encompassing only the upstream promoter region were PCR-amplified and cloned into the pGPTV–BAR binary vector (Becker *et al.*, 1992). The resulting constructs are referred to as *pSPL8:GUS*, *pSPL2:GUS*, *pSPL10:GUS*, *pSPL11:GUS*, *pSPL6:GUS* and *pSPL13:GUS*. Oligonucleotides used for amplification of the promoter regions are listed in Table S1. Confirmed correct constructs were transformed into wild-type plants by the floral-dip method (Clough and Bent, 1998).

Histology and microscopy

GUS staining was performed as described by Sieburth and Meyerowitz (1997) in the presence of 0.5 mM potassium ferro- and ferricyanide. Pollination experiments and aniline blue staining were performed as previously described (Jiang *et al.*, 2005). Embedding and sectioning of flowers as well as seed set determination were performed as described by Xing *et al.* (2010), and Alcian blue staining of the thin sections was performed as described by Sessions and Zambryski (1995). For scanning electron microscopy, we followed the protocol described by Unte *et al.* (2003).

NPA treatment

NPA (1–*N*–naphthylphthalamic acid; Duchefa Biochemie B.V., Haarlem, The Netherlands; catalogue number N0926.0250, http://www.duchefa-biochemie.nl/) treatment was performed as previously described by Sohlberg *et al.* (2006).

Real-time quantitative RT–PCR

Wild-type roots were collected from 18-day-old seedlings grown on MS medium. Rosette leaves, cauline leaves, stem and siliques were sampled from 6-week-old plants. Inflorescence tips without open flowers were harvested from 30-day-old plants. RNA isolation and quantitative RT–PCR were performed as described by Xing *et al.* (2010).

ACKNOWLEDGEMENTS

We thank the Weigel laboratory (Max Planck Institute for Developmental Biology, Tübingen, Germany) for providing the *35S:MIR156b* transgenic line, Cristina Ferrándiz (Universidad Politécnica Valencia, Spain) and Eva Sundberg (Uppsala BioCenter Swedish University, Sweden) for the *pYUC4:GUS* line and sharing other plant materials, and Marty Yanofsky (University of California San Diego, La Jolla, USA) and David Smyth (Monash University, Melbourne, Australia) for the *pHEC2:GUS* and *pSPT:GUS* lines, respectively. Arne Grande (Max Planck Institute for Plant Breeding Research, Cologne, Germany) is thanked for his help with scanning electron microscopy imaging, and John Alvarez (Department of Plant Biology, University of California Davis, USA) is thanked for sharing preliminary data concerning the expression of *SPL8*. This project was funded by the Deutsche Forschungsgemeinschaft through Collaborative Research Center SFB572.

SUPPORTING INFORMATION

Additional Supporting Information may be found in the online version of this article.

Figure S1. Identification of T–DNA insertion mutants.

Figure S2. Trichome visible inside a cleared *35S:MIR156b spl8–1* double mutant ovary.

Figure S3. *pHEC2:GUS* expression in inflorescences of *spl* mutants.

Figure S4. Expression pattern of *pSPT:GUS* in *ett* and *spl8* mutants.

Table S1. Oligonucleotide primer sequences.

REFERENCES

Alvarez, J. and Smyth, D. R. (1998) Genetic pathways controlling carpel development in *Arabidopsis thaliana*. *J. Plant. Res.*, **111**, 295–298.

Alvarez, J. and Smyth, D. R. (1999) *CRABS CLAW* and *SPATULA*, two Arabidopsis genes that control carpel development in parallel with *AGAMOUS*. *Development*, **126**, 2377–2386.

Alvarez, J. P., Goldschmidt, A., Efroni, I., Bowman, J. L. and Eshed, Y. (2009) The *NGATHA* distal organ development genes are essential for style specification in Arabidopsis. *Plant Cell*, **21**, 1373–1393.

Angenent, G. C., Franken, J., Busscher, M., van Dijken, A., van Went, J. L., Dons, H. J. and van Tunen, A. J. (1995) A novel class of MADS box genes is involved in ovule development in petunia. *Plant Cell*, **7**, 1569–1582.

Balanza, V., Navarrete, M., Trigueros, M. and Ferrandiz, C. (2006) Patterning the female side of Arabidopsis, the importance of hormones. *J. Exp. Bot.*, **57**, 3457–3469.

Becker, D., Kemper, E., Schell, J. and Masterson, R. (1992) New plant binary vectors with selectable markers located proximal to the left T-DNA border. *Plant Mol. Biol.*, **20**, 1195–1197.

Clough, S. J. and Bent, A. F. (1998) Floral dip: a simplified method for *Agrobacterium*-mediated transformation of *Arabidopsis thaliana*. *Plant J.*, **16**, 735–743.

Colombo, M., Brambilla, V., Marcheselli, R., Caporali, E., Kater, M. M. and Colombo, L. (2010) A new role for the *SHATTERPROOF* genes during Arabidopsis gynoecium development. *Dev. Biol.*, **337**, 294–302.

Crawford, B. C. W. and Yanofsky, M. F. (2008) The formation and function of the female reproductive tract in flowering plants. *Curr. Biol.*, **18**, R972–R978.

Crawford, B. C. W. and Yanofsky, M. F. (2011) *HALF FILLED* promotes reproductive tract development and fertilization efficiency in *Arabidopsis thaliana*. *Development*, **138**, 2999–3009.

Crawford, B. C. W., Ditta, G. and Yanofsky, M. F. (2007) The *NTT* gene is required for transmitting-tract development in carpels of *Arabidopsis thaliana*. *Curr. Biol.*, **17**, 1101–1108.

Eklund, D. M., Ståldal, S., Valsecchi, I. *et al.* (2010) The *Arabidopsis thaliana* STYLISH1 protein acts as a transcriptional activator regulating auxin biosynthesis. *Plant Cell*, **22**, 349–363.

Ferrándiz, C., Pelaz, S. and Yanofsky, M. F. (1999) Control of carpel and fruit development in Arabidopsis. *Annu. Rev. Biochem.*, **68**, 321–354.

Ferrándiz, C., Fourquin, C., Prunet, N., Scutt, C. P., Sundberg, E., Trehin, C. and Vialette-Guiraud, A. C. M. (2010) Carpel development. *Adv. Bot. Res.*, **55**, 1–73.

Gremski, K., Ditta, G. and Yanofsky, M. F. (2007) The *HECATE* genes regulate female reproductive tract development in *Arabidopsis thaliana*. *Development*, **134**, 3593–3601.

Heisler, M. G., Atkinson, A., Bylstra, Y. H., Walsh, R. and Smyth, D. R. (2001) *SPATULA*, a gene that controls development of carpel margin tissues in Arabidopsis, encodes a bHLH protein. *Development*, **128**, 1089–1098.

Huijser, P. and Schmid, M. (2011) The control of developmental phase transitions in plants. *Development*, **138**, 4117–4129.

Jiang, L., Yang, S. L., Xie, L. F., Puah, C. S., Zhang, X. Q., Yang, W. C., Sundaresan, V. and Ye, D. (2005) *VANGUARD1* encodes a pectin methylesterase that enhances pollen tube growth in the Arabidopsis style and transmitting tract. *Plant Cell*, **17**, 584–596.

Kuusk, S., Sohlberg, J. J., Long, J. A., Fridborg, I. and Sundberg, E. (2002) *STY1* and *STY2* promote the formation of apical tissues during Arabidopsis gynoecium development. *Development*, **129**, 4707–4717.

Liljegren, S. J., Ditta, G. S., Eshed, Y., Savidge, B., Bowman, J. L. and Yanofsky, M. F. (2000) *SHATTERPROOF* MADS-box genes control seed dispersal in Arabidopsis. *Nature*, **404**, 766–770.

Lord, E. M. and Russell, S. D. (2002) The mechanisms of pollination and fertilization in plants. *Annu. Rev. Cell Dev. Biol.*, **18**, 81–105.

Moreno, M. A., Harper, L. C., Krueger, R. W., Dellaporta, S. L. and Freeling, M. (1997) *liguleless1* encodes a nuclear-localized protein required for induction of ligules and auricles during maize leaf organogenesis. *Genes Dev.*, **11**, 616–628.

Nemhauser, J., Feldman, L. and Zambryski, P. (2000) Auxin and *ETTIN* in *Arabidopsis* gynoecium morphogenesis. *Development*, **127**, 3877–3888.

Pekker, I., Alvarez, J. P. and Eshed, Y. (2005) Auxin response factors mediate *Arabidopsis* organ asymmetry via modulation of KANADI activity. *Plant Cell*, **17**, 2899–2910.

Schmid, M., Davison, T. S., Henz, S. R., Pape, U. J., Demar, M., Vingron, M., Schölkopf, B., Weigel, D. and Lohmann, J. (2005) A gene expression map of Arabidopsis development. *Nat. Genet.*, **37**, 501–506.

Schwab, R., Palatnik, J. F., Riester, M., Schommer, C., Schmid, M. and Weigel, D. (2005) Specific effects of microRNAs on the plant transcriptome. *Dev. Cell*, **8**, 517–527.

Sessions, R. A. and Zambryski, P. C. (1995) Arabidopsis gynoecium structure in the wild type and in *ettin* mutants. *Development*, **121**, 1519–1532.

Sessions, A., Nemhauser, J. L., McColl, A., Roe, J. L., Feldmann, K. A. and Zambryski, P. C. (1997) *ETTIN* patterns the Arabidopsis floral meristem and reproductive organs. *Development*, **124**, 4481–4491.

Sieburth, L. E. and Meyerowitz, E. M. (1997) Molecular dissection of the *AGAMOUS* control region shows that *cis* elements for spatial regulation are located intragenically. *Plant Cell*, **9**, 355–365.

Sohlberg, J. J., Myrenas, M., Kuusk, S., Lagercrantz, U., Kowalczyk, M., Sandberg, G. and Sundberg, E. (2006) *STY1* regulates auxin homeostasis and affects apical–basal patterning of the Arabidopsis gynoecium. *Plant J.*, **47**, 112–123.

Trigueros, M., Navarrete-Gómez, M., Sato, S., Christensen, S. K., Pelaz, S., Weigel, D., Meyerowitz, E. M. and Ferrándiz, C. (2009) The *NGATHA* genes direct style development in the Arabidopsis gynoecium. *Plant Cell*, **21**, 1394–1409.

Unte, U. S., Sorensen, A. M., Pesaresi, P., Gandikota, M., Leister, D., Saedler, H. and Huijser, P. (2003) *SPL8*, an SBP-box gene that affects pollen sac development in Arabidopsis. *Plant Cell*, **15**, 1009–1019.

Wang, J. W., Schwab, R., Czech, B., Mica, E. and Weigel, D. (2008) Dual effects of miR156-targeted *SPL* genes and *CYP78A5/KLUH* on plastochron length and organ size in *Arabidopsis thaliana*. *Plant Cell*, **20**, 1231–1243.

Xing, S., Salinas, M., Höhmann, S., Berndtgen, R. and Huijser, P. (2010) miR156-targeted and nontargeted SBP-box transcription factors act in concert to secure male fertility in Arabidopsis. *Plant Cell*, **22**, 3935–3950.